HHS Public Access

Author manuscript

Anesthesiology. Author manuscript; available in PMC 2019 October 01.

Published in final edited form as:

Anesthesiology. 2018 October ; 129(4): 733–743. doi:10.1097/ALN.0000000000002342.

The breakdown of neural function under isoflurane anesthesia: in vivo, multineuronal imaging in *C. elegans*

Mehraj Awal, BS,
Research Assistant, Department of Physiology and Biophysics, Boston University School of Medicine, Boston, MA, USA

Doug Austin, BA,
Research Technician, Department of Physiology and Biophysics, Boston University School of Medicine, Boston, MA, USA

Jeremy Florman, BA,
Research Assistant, Department of Neurobiology, University of Massachusetts Medical School, Worcester, MA

Mark Alkema, PHD,
Associate Professor of Neurobiology, University of Massachusetts Medical School, Worcester, MA

Christopher V Gabel, PhD[#], and
Associate Professor of Physiology and Biophysics, Pharmacology and Experimental Therapeutics, Boston University School of Medicine, Photonics Center, Boston University, Boston, MA, USA

Christopher W Connor, MD, PHD[#]
Assistant Professor of Anesthesiology, Department of Anesthesiology, Peri-operative and Pain Medicine, Brigham and Women's Hospital, Boston, MA, USA. Research Associate Professor of Physiology and Biophysics, Boston University, Boston, MA, USA

Abstract

Background—Prior work on the action of volatile anesthetics has focused at either the molecular level, or bulk neuronal measurement such as EEG or fMRI. There is a distinct gulf in resolution at the level of cellular signaling within neuronal systems. We hypothesize that anesthesia is caused by induced dyssynchrony in cellular signaling, rather than suppression of individual neuron activity.

Corresponding Author: Dr. Christopher W Connor, Department of Anesthesiology, Perioperative and Pain Medicine, Brigham and Women's Hospital, 75 Francis Street, CWN L1, Boston, MA 02115, cconnor@bwh.harvard.edu.
[#]These authors contributed equally to the work

Conflict of Interest/Financial Disclosures: None

Prior Presentations: Presented in part as a poster for the session "Experimental Neurosciences: Exploring Novel Techniques and Molecules" at the 2017 Annual Meeting of the American Society of Anesthesiologists, October 21st 2017, Boston, MA.
Presented in part as a poster at the 21st International C. *elegans* Conference, June 21st – 25th 2017, UCLA, Los Angeles CA.

Contributions: MRA, CWC, and CVG designed the study, developed the methodology, performed the analysis, and wrote the manuscript. MRA and DA collected the data. MJA and JF constructed *C. elegans* strains. CVG and CWC developed new analytic tools and supervised the research.

Methods—Employing confocal microscopy and *C. elegans* expressing the calcium-sensitive fluorophore GCaMP6s in specific command neurons, we measure neuronal activity non-invasively and in parallel within the behavioral circuit controlling forward and reverse crawling. We compare neuronal dynamics and coordination in a total of 31 animals under atmospheres of 0%, 4% and 8% isoflurane.

Results—When not anesthetized, the interneurons controlling forward or reverse crawling occupy two possible states, with the activity of the "reversal" neurons AVA, AVD, AVE and RIM strongly inter-correlated, and the "forward" neuron AVB anti-correlated. With exposure to 4%vol isoflurane and onset of physical quiescence, neuron activity wanders rapidly and erratically through indeterminate states. Neuron dynamics shift toward higher frequencies and neuron pair correlations within the system are reduced. At 8%vol isoflurane physical quiescence continues as neuronal signals show diminished amplitude with little correlation between neurons.

Neuronal activity was further studied using statistical tools from information theory to quantify the type of disruption caused by isoflurane. Neuronal signals become noisier and more disordered, as measured by an increase in the randomness of their activity (*Shannon entropy*). The coordination of the system - measured by whether or not information exhibited in one neuron is also exhibited in other neurons (*multi-information*) - decreases significantly at 4%vol isoflurane ($p = 0.00015$) and 8%vol isoflurane ($p = 0.0028$).

Conclusions—The onset of anesthesia corresponds with high-frequency randomization of individual neuron activity coupled with induced dyssynchrony and loss of coordination between neurons that disrupts functional signaling.

Introduction

Volatile anesthetics produce all characteristics of general anesthesia including unconsciousness, amnesia, analgesia and muscle relaxation. In this physiological state, the experience, memory and physical response to excruciating pain are lost. However, it is not understood how this state is produced within intact neuronal systems such that sensory awareness is ablated while essential physiology is preserved. To date, research has proceeded along essentially two tracks: either gross measurement of neuronal activity in entire regions of the brain using fMRI and EEG (which are fundamentally limited by resolution), or analysis at the molecular level looking for specific targets for volatile anesthetics. Thus a critical gap exists in our knowledge regarding the scale on which the effects of volatile anesthetics are analyzed. As stated by Hudson in this journal –there is a commanding need to "seek bridges between systems- and cellular-level models" of anesthesia[1]. Here multi-neuronal imaging is employed within the simple and highly characterized nervous system of *C. elegans* to address these fundamental questions.

The hermaphrodite *C. elegans* (Figure 1) nervous system consists of exactly 302 neurons[2]. Decades of research have defined numerous neuronal circuits within this system that control behaviors ranging from simple body movement to memory and complex search strategies[3–5]. *C. elegans* is established as a model system in anesthesiology[6], displaying distinct stages of gross behavior under anesthesia similar to humans[7]. In particular *C. elegans'* amenable genetics have facilitated the study of anesthetic action at the molecular

level, identifying genetic mutations that alter anesthetic susceptibility[6]. Finally, *C. elegans* is a powerful system for *in vivo* neuronal imaging in which transgenically expressed fluorescent calcium indicators, such as GCaMP, optically report individual neuron activity. This technique permits imaging in real-time, *in vivo*, and at resolutions capable of simultaneously capturing the activity of individual neurons within entire populations of complex interconnected neuronal networks[8–11]. Through this real-time measurement of individual neuron activity, we seek to understand how subtle modifications in discrete neuronal dynamics lead to gross but reversible functional defects at the level of the overall nervous system that result in analgesia and physical quiescence.

In this study, the effect of isoflurane on the interneuron circuit in *C. elegans* that controls its reversal behavior is analyzed. Well-characterized, mutually antagonistic command interneurons control a behavioral switch between continual forward movement and spontaneous or stimulus-evoked reversal events[3,12] (Figure 1D). Sensory neurons project onto these interneurons to elicit appropriate behavioral responses (e.g. reversal in response to anterior touch). The system resembles a binary flip-flop circuit in which the cross-inhibitory neuron groups force the system into one of two states: forward or backward crawling[12]. By optically measuring the activity of multiple neurons within this well-understood circuit at varying levels of anesthesia, the effect on the system's function can be directly measured. Specifically, the hypothesis is tested that anesthesia is caused by induced dyssynchrony between neurons, rather than a suppression of individual neuron activity. This dyssynchrony is reflected in increased neuronal activity and decreased coordination between neurons that impairs the circuit's capacity to assume distinct behavioral states.

Methods

Strains

C. elegans strains were cultivated at 20°C following standard procedures (on NGM agar seeded with Escherichia coli OP50 as a food source). All imaging experiments were performed on young adult hermaphrodites (Figure 1A), using the transgenic strains QW1217 (*zfIs124[Prgef-1::GCaMP6s]; otIs355[Prab-3::NLS::tagRFP]*) expressing pan-neuronal GCaMP and nuclear-localized RFP in all neurons in the worm (Figure 1B), and QW1574 (*lite-1(ce314), zfis146[nmr-1::NLSwCherry::SL2::GCaMP6s, lim-4(-3328--2174)::NLSwCherry::SL2::GCaMP6s, lgc-55(-120-773)::NLSwCherry::SL2::GCaMP6s, npr-9::NLSwCherry::SL2::GCaMP6s] #18.9* (from *zfex696*)), expressing GCaMP-6s and nuclear-localized RFP in the circuit neurons (Figure 1C). The wild isolate N2 and the transgenic strain CX2610 (*kyIs30 [glr-1::GFP + lin-15(+)]*), expressing GFP under the *glr-1* promoter, were obtained from the Caenorhabditis Genetics Center (CGC, University of Minnesota).

Behavioral Assays

The behavioral experiments were performed in an experimental chamber containing an atmosphere of isoflurane in humid air. Liquid isoflurane was instilled into the chamber via a Harvard Apparatus syringe pump (Holliston, MA) and allowed to vaporize in a controlled environment at 20°C. The atmosphere in the chamber was continuously sampled for

isoflurane with an Ohmeda 5250 RGM Anesthesia Monitor (GE Healthcare, Madison, WI). The concentration of isoflurane in the atmosphere within the chamber was titrated by varying the rate of instillation at the syringe pump.

The motion of the worms while crawling on the surface of an agar Petri dish was tracked with a CCD camera, with images at a rate of 2 fps. The resulting movies were analyzed using MATLAB (The Mathworks, Natick, MA) to calculate the average speed and incidence of reversals for each tracked worm (Figure 2). Reversals were induced by the application of a vibration stimulus to the Petri dish actuated via a small motor attached to the chamber and control using Labview (National Instruments Corporation, Austin, TX). The duration of the vibration was tuned to 0.05 seconds, which induced reversals in 80% of worms in a control population. Vibration stimuli were separated by more than 10 minutes to avoid habituation to the stimulus.

Confocal Imaging

8% agarose was melted and pressed into small thin pads against glass slides. The slides were placed into the above-described experimental chamber and exposed to isoflurane for 1 hour at either 4%vol or 8%vol in humid air. A single worm was then placed onto each agarose pad in the chamber, and exposed for 3 hours to either 4% or 8% isoflurane, at room temperature (climate controlled, 20°C). In turn, each slide was removed and sealed promptly with a glass slip and wax. This preparation is stable for at least 1 hour; imaging was performed within 7 minutes of mounting the worms in each case, well before the possibility of recovery from exposure to the isoflurane.

Neuronal imaging was performed using the QW1574 strain expressing GCaMP-6s and nuclear-localized RFP in select interneurons. A Zeiss 700 confocal with a 40× oil objective (Carl Zeiss Microscopy, Peabody, MA) was used to image each worm for up to 10 minutes, with interleaved illumination with a 488 nm laser at 1% power to image GCaMP-6s in the green and a 555 nm laser at 2% power to image NLSwCherry in the red. Image sequences were acquired at 2 fps, using Nyquist-optimal resolution and a 2 Airy Unit pinhole (depth of field 1.8 um). The environment was maintained at 20°C during imaging. This procedure was repeated for each slide. At least nine different worms were imaged at each condition. The intensity of GCaMP6s fluorescence varies with cytosolic calcium concentration giving a well-established optical readout of neuronal activity[13]. *C. elegans* neurons typically display slow transient changes in activity and do not produce rapid action potentials[14,15]. Thus a frame rate of 2fps sufficiently captured interneuron dynamics while limiting photo-bleaching to allow for extended imaging, ~10 min. Green Fluorescent Protein (GFP) is a fluorophore similar to CGaMP-6 but calcium insensitive. Animals expressing GFP in the neurons of interest were therefore employed in control experiments to ascertain the degree of baseline noise in the imaging technique.

Image Analysis

Neurons were identified using the nucleus-specific red fluorescent tag, NLSwCherry, and the known anatomical location in the worm head. Motion compensation for any residual activity in the worm was achieved by manual identification of each neuron of interest in each image

frame. The GCaMP signal for calcium fluorescence in the soma of each identified neuron was then captured over the entire time course of imaging (5–10 min). Fluorescence intensity, F(t), for each frame was measured as the average pixel value across the region of interest (i.e. the cell soma) minus the average pixel value in a background region selected close to, but not encompassing, any fluorescent neurons. The example calcium traces are given in Figure 3, displayed as $\Delta F/F_o$ where F_o is calculated as the average fluorescence value across the entire trial and $\Delta F = F\text{-}F_o$. Normalized traces (normalized to the mean value of the largest 5% of data points in that trace) were used to generate the associated activity histograms by binning all normalized intensity values for each neuron across all worms at that condition. The number of movies analyzed for each condition is stated in Table 1A. One movie was not analyzed for neuronal function because significant physical drift precluded analysis and was not included in the reported *n*. We report AVA, AVD, AVE and RIM for all worms and in our statistical analysis (correlations, power spectrum and entropies), so that the neurons used are consistent for analysis under all conditions. The continuous identification of AVB under anesthesia is made challenging by relatively weak expression of the NLSwCherry RFP nuclear marker under the lgc-55 promoter in the QW1574 worm. Thus the archetypal response of AVB is displayed for the awake worm alone, Figure 3A, 4A, but not included in further analysis.

Subsequent analysis in Figures 4, 5 employed the time-differential of neuron traces (calculated using total-variation regularization[16]). This technique most effectively reports neuron co-activation (i.e. simultaneous activation or de-activation of independent neuron traces), as well as the signal dynamics most similar to EEG recordings (see below). Specific neuron-neuron correlations, displayed in the correlation heatmaps in Figure 4A–C, were calculated between the time-differential traces of those neurons for each worm and then averaged across all worms at that condition for that neuron pair. To measure average correlation under each condition, Figure 4D, all correlation measurements at each condition were pooled across all neuron pairs to give an average absolute correlation value from which statistical comparisons could be made (one-way ANOVA, with pairwise comparisons tested using a Tukey adjustment).

The fluorescence traces were further analyzed by deriving the power spectra of the time-differential of neuron dynamics to produce a representation of activity that is analogous to an EEG spectrogram in higher animals. EEGs effectively measure the bulk time-differential of neuron activity given that the local electrical field potential is proportional to the current flow at the source[17] for a given distance and volume conductance. The optical brightness of the GCaMP signal is therefore differentiated with respect to time in order to estimate an equivalent signal to the EEG. The power spectrum of each neuron was first calculated separately and then averaged across all neurons at that condition. Figure 5, insert shows the cumulative power spectrum calculated from the average power spectrum by plotting the normalized power above the indicated frequency.

Statistics and Analysis by Information Theory

The behavior of a network can be analyzed in terms of its information-theoretic properties[18]. The cornerstone of this technique is to analyze the behavior of the network in terms of its

Shannon entropy. Larger Shannon entropy indicates a noisier, or more randomized, system with less organized information content. This approach is similar to the analysis of the human EEG under anesthesia by directed information transfer[19]. The state of each neuron is quantized into four quartiles (i.e. full-off, intermediate-off, intermediate-on, and full-on), and the associated information entropy is calculated using the formula:

$$H(x) = \sum_{i=1}^{k} p_i(x) \log_2 \frac{1}{p_i(x)} \quad \text{(Eq 1)}$$

where $p(x)$ is the probability of the neuron x being in each of the $k = 4$ possible quantized states. For example, if the neuron AVA were to behave purely randomly, then each p_i(AVA) would be equal to 0.25. Therefore the entropy H(AVA) would be $4 \times 0.25 \times \log_2(1/0.25) = 2$ bits, which is the maximum obtainable value. Increasingly organized behavior will progressively reduce the entropy below 2. In addition to considering the behavior of the neurons individually, the joint entropy of their behavior can also be measured as H(AVA,AVD,AVE,RIM) by considering the probability of each of the $4^4 = 256$ joint states of activation that may occur (in general, if n neurons are allowed to have k states, there are k^n joint states and therefore k should be kept as small as is practicable). Joint entropy measures the degree to which the neurons represent distinct information. In this example, if all 4 neurons were to behave entirely randomly and independently, the joint entropy would be 8 bits. If only 1 neuron behaves randomly and the other 3 neurons replicate its state exactly, then the joint entropy would be only 2 bits.

The strength of the interactions within the neuronal network can be assessed using the *multi-information* M[20], which is the difference between the sum of the individual entropies and their joint entropy:

$$M = \left(\sum_{j=1}^{n} H\left(x_j\right) \right) - H\left(x_1, x_2, \ldots, x_n\right) \quad \text{(Eq 2)}$$

For a system in which neurons behave entirely at random and independently, the sum of the individual entropies and their joint entropy cancel out, leaving an M of 0. As the coordination between neurons increases, their joint entropy decreases, and so M increases. A peak in the multi-information, $M_{\max,}$ is achieved when the network acts in a purely mechanistic and coordinated manner such that the behavior of each neuron can be predicted perfectly from one individual neuron at one time point as if by clockwork. Here the number of distinct states of the system drops and the joint entropy reduces to just that of the maximal single neuronal entropy, max $H(x)$. The peak multi-information $M_{\max}$ is then defined as:

$$M_{\max} = \left(\sum_{j=1}^{n} H\left(x_j\right) \right) - \max_j H\left(x_j\right) \quad \text{(Eq 3)}$$

The multi-information M within the neuronal network can now be expressed more intuitively as a percentage of M_{max}, so that 0% represents no coordination between neurons and 100% represents a perfectly mechanical interaction as defined above. The assumptions underlying the use of parametric statistics were considered and that the use of mean (SD), ANOVA, and t-tests are appropriate.

Results

Behavioral Analysis

Figure 2 illustrates the gross physical behavior of *C. elegans* under exposure to increasing levels of isoflurane. These results are comparable to those of previous studies[7]. Figure 2A shows the average crawling speed of the worm with increasing levels of exposure to an isoflurane-containing atmosphere. Under control conditions (i.e. 0% isoflurane), *C. elegans* crawl in linear or gently curving tracks interrupted by short reversals or brief periods of large angle turning. Exposure to isoflurane produces an agitated coiling behavior in which rapid and irregular changes in direction become apparent and overall speed of the animal decreases, Figure 2B. Qualitatively, this onset of undirected and purposeless movement is evocative of a second-stage response to volatile anesthetic agents. Further increases in the level of isoflurane produce further slowing in overall motion and eventual quiescence.

C. elegans reversals occur spontaneously, but can also be induced by a global mechanical stimulation, generated by physical buzzing of the Petri dish. Figure 2C illustrates the progressive abolition of this response under exposure to increasing concentrations of isoflurane. Sustained exposure to an isoflurane-containing atmosphere at a concentration of 4%vol produces worms that are largely quiescent and unresponsive to noxious stimuli. These gross changes in physical behavior are maintained with deepening anesthetic levels (>4%). Isoflurane concentrations of 8%vol are a practical limit on the deepest plane of anesthetic exposure; the experimental animals do not reliably recover from greater exposure.

Neuronal Imaging

The operation of the command interneuron circuitry and its functional control of the forward and reverse crawling were measured. This is accomplished through the simultaneous fluorescent imaging of calcium sensitive G-CaMP6s expressed in a subset of neurons (AVA, AVB, AVD, AVE, RIM, Figure 1C,D) to optically measure individual neuron activity. In awake, freely-moving *C. elegans*, reversal events consist of the simultaneous activation of AVA, AVD, AVE and suppression of AVB[12]. Likewise, the transition from backward to forward movement consists of activation of AVB and suppression of AVA, AVD, AVE. RIM acts as an interneuron between these two groups[21]. Figure 3A displays an example trace of this activity in an awake animal (0% isoflurane) over 10 minutes. The spontaneous reversal behavior is clearly represented in the neuronal state of the system even though the animal is physically immobilized for confocal microscopy. This behavior was consistent across the population of imaged awake animals and reflected in the distributions of normalized neuronal signals (Figure 3A, right). AVA, AVE and RIM activity distributions are concentrated near the extremes of their dynamic range, i.e. they are either “ON” or “OFF”. While AVD and AVB displayed similar behavior their activation amplitude varies more

widely with time and thus the overall amplitude distributions are more evenly distributed across their dynamic range.

The degree of coordination in the circuit can be quantified by measuring the correlation in activity (i.e. simultaneous activation and suppression) between neuron pairs across all awake animals. This is displayed in Figure 4A as a correlation heatmap with color indicating the degree of correlation between two neuron types (red correlated, blue anti-correlated, white no correlation). Strong positive correlation is seen between the “reversal” neurons of AVA, AVD and AVE, as well as RIM, which are anti-correlated with the “forward” neuron, AVB, in the awake worm. These correlations are calculated on a per-worm basis, so that a mean correlation and standard deviation can be given for each neuron-neuron pair. The correlation of a neuron with itself is 1.0 by definition.

The effect of exposure to increasing concentrations of isoflurane on the temporal operation of the command interneuron circuitry was measured. Exposure to 4%vol isoflurane, at which worms are largely immobile and unresponsive, produces neuronal dynamics in which the neuronal network no longer settles to one of two distinct, binary outputs (Figure 3B, left). Rather the system appears to oscillate irregularly through intermediate states. This is reflected in the normalized activity distributions that are now evenly spread across the neuron’s dynamic range (Figure 3B, right). Furthermore, there is a profound impairment of the strong neuron-neuron correlations observed in awake animals (Figure 4B). By taking the absolute correlation values across all neuron pairs for all trials at each level of isoflurane exposure, an average correlation magnitude for that level of isoflurane can be calculated, Figure 4D. This generalized measurement of circuit correlation drops significantly between 0% and 4% isoflurane ($p < 0.0001$).

In a state of deep anesthesia, a more general suppression of neuronal activity is seen. At 8% vol isoflurane the overall amplitude of neuronal dynamics are greatly diminished (Figure 3C, left) and the normalized amplitudes become evenly distributed across its dynamic range (Figure 3C, right). Such measurements are similar to those obtained from control measurements made in GFP-expressing neurons (GFP is a stable fluorophore which does not change in fluorescent intensity due to neuronal activity). This suggests that the majority of the neuron activity has been eliminated leaving only the baseline noise of the imaging technique. The average correlation across neuron pairs at 8% is significantly lower than that of awake animals ($p < 0.0001$, Figure 4D). The reduction in overall neuronal activity at 8% compared to that of 4% isoflurane produces a small, but statistically significant ($p = 0.0039$) increase in the mean correlation coefficient as neurons cease to fluctuate relative to each other.

Spectral and Informational Analysis

To further quantify the changes of neuronal activity under anesthesia, a power spectral analysis of the measured fluorescence signals was performed. Such analysis follows traditional power spectral analysis of EEG measurements in human patients[22] but at the level of single neuron activity rather than that of bulk measurements across large regions of the brain. Figure 5 displays the average power spectrum of all neuron activity measured at each condition as well as that of GFP controls (see methods). Most of the power in the awake

neuronal activity (0% isoflurane, blue line) is below ~0.2 Hz, reflecting the slow dynamics of switching between organized forward and reverse states (seen in Figure 3A). At 4% isoflurane (black line) there is a distinct shift toward higher frequency dynamics (> 0.2 Hz) and a relative reduction of power at lower frequencies. This shift is highlighted by the cumulative power spectrums of 0% and 4% isoflurane plotted in the Figure 5 insert and reflects the increase in high frequency random noise observed in the neuron traces at 4% isoflurane (seen in Figure 3B). At deeper levels of anesthesia (8% isoflurane, red line) there is a dramatic drop in overall power corresponding to the decrease in signal amplitude seen in Figure 3C, generating a power spectrum similar to GFP control measurements (green line).

Information theory has proven useful in analysis of brain activity as measured by EEG[19]. By discretizing the calcium traces of each neuron into quartiles, the degree of disorder in the neuronal activity can be quantified by its Shannon entropy (see Methods). Table 1A shows that exposure to isoflurane causes a marked increase in the entropy of each of the observed neurons as their organized behavior is lost. Exposure to isoflurane also markedly increases the joint entropy of the neurons H(AVA,AVD,AVE,RIM) that measures the disorder of the system as a whole. The strength of the neuronal interactions can then be assessed by calculating the *multi-information, M*, of the system (see Methods). The multi-information of the four measured neurons is relatively high in the awake animal indicating highly structured activity. It falls markedly on exposure to isoflurane, both in absolute terms and in proportion to M_{max}. The entropy calculations in Table 1A are based on the pooled data of the n worms at each level of isoflurane in order to maximize the accuracy of the sampling of the underlying probability distributions. When M is calculated on the basis of each individual worm as shown in Table 1B, a two-sample t-test confirms that the multi-information at 0% isoflurane is different from the multi-information at both 4% and 8% isoflurane with statistical significance ($p = 0.00015$ and $p = 0.0028$ respectively), but that the multi-information at 4% and 8% isoflurane are not statistically different from each other ($p = 0.093$).

Discussion

The complete *C. elegans* neuro-connectome was established in the 1980s[2]. Subsequent studies have determined the functional activity of sub-circuits controlling a range of behaviors from basic body movement to complex avoidance and search strategies that involve rudimentary forms of learning and memory. Anesthetic research in *C. elegans* has revealed an analogous behavioral response to volatile anesthetics similar to that of higher-order organisms, as well as numerous molecular mechanisms that alter its anesthetic susceptibility. In particular, certain mitochondrial mutations increasing susceptibility appear to have direct corollaries in higher organisms: *gas-1* (*C. elegans*), *Ndfus4* (mice) and Leigh Syndrome (humans)[23]. Here we establish *C. elegans* as a uniquely simple and powerful system for the functional imaging and study of neuronal systems under anesthesia. The simplicity and clarity of *C. elegans* neuronal architecture and function, and its accessibility for advanced multi- and pan-neuronal imaging, can serve as the missing link between the molecular and system-wide effects of volatile anesthetics.

The application of isoflurane has a distinct effect on both the activity of individual neurons as well as coordination of the system. At 4%vol isoflurane, *C. elegans* display behavior akin to the third stage of anesthesia with minimal spontaneous movement and no response to external stimulation (Figure 2). This quiescence however is not due to the simple silencing of neuronal activity as the individual command interneurons remain highly active (Figure 3B, 5). The neuronal activity is altered compared to awake animals (Figure 3A) in that they no longer maintain distinct on/off states but show apparently random fluctuations in amplitude. This observation is quantified by the power spectrum analysis in Figure 5. The shift to higher frequency dynamics demonstrates that the highly organized forward-reverse impulses, represented in the low frequency power in the innate state, are lost to high frequency “noise” upon the application of isoflurane. In addition, the coordination between neurons as part of the command neuron circuitry is clearly lost relative to the awake state. The correlation heatmaps in Figure 4 show that AVA, AVD, AVE and RIM lose their strong correlation with each other. Likewise the average degree of correlation at 4% isoflurane drops significantly compared to awake animals, Figure 4D. Therefore, the primary cause of this state of anesthesia is not the suppression of individual neuron activity but rather the loss of coordination between neurons within a well-defined circuit.

At deeper levels of anesthesia, 8%vol isoflurane, the neuronal signals remain randomized but now with diminished amplitude and a lack of distinct activation events (Figure 3C). Likewise coordination between neurons remains minimal, similar to that at 4% isoflurane, as shown in the correlation heat map and average correlation value (Figure 4C,D). The spectrum analysis in Figure 5 shows a substantial decrease in signal power and a spectrum comparable to control measurements made of neurons expressing a non-responsive GFP fluorophore. Thus at this level the animals appear to have reached the deep plane of anesthesia resulting in neuronal quiescence akin to an isoelectric state in human patients.

Information theory further quantifies how the state of anesthesia results in reduced neuronal coordination within the system. Table 1A shows that exposure to isoflurane causes a marked increase in the entropy of the observed neurons as the organized behavior of each is lost. Exposure to isoflurane also markedly increases the joint entropy of the system as a whole (Table 1A). The strength of the interactions within the neuronal network can then be assessed using the *multi-information M*[20], measured as the difference between the individual entropies and the joint entropy in the network. Completely independent neuronal activity would result in an M of 0, whereas a network that is completely coordinated would have the highest possible M. Table 1A shows that the multi-information of the four measured neurons is relatively high in awake animals, reflecting the high degree of organization in the innate system and then falls markedly on exposure to isoflurane. It is interesting to note that both moderate and deep anesthesia results in comparable changes in entropy and multi-information compared to the awake state. Moreover, these changes mimic the reduction in neuron pair correlations measured in Figure 4 at both moderate and deep anesthesia. The physical signs of the onset of anesthesia therefore coincide with decreased correlation between neurons, an increase of entropy in the neuronal dynamics and loss of multi-information (i.e. the loss of coordination) within the network. These results are consistent with the initial hypothesis as they quantify the degree to which the system loses its innate coordination under anesthesia.

While the purpose of the imaging technique presented here is to measure the behavior of multiple individual neurons under isoflurane anesthesia, it is also instructive to consider how these findings are compatible with those from bulk recording techniques such as EEG or fMRI. The signal from many thousands of proximate neurons in these techniques can be expected to be additive, such that uncorrelated activations at higher frequencies would cancel out and lead to a *reduction* in the higher frequencies of bulk measurement power spectra. Thus the underlying randomization of individual neuron activity could result in the apparent silencing or suppression of a population of neurons while individual neurons remain active or even hyperactive, below the sensing resolution of these bulk techniques. Regardless, these measurements illustrate that action of individual neurons and defined neuronal systems under anesthesia can be dramatically different than what is perceived through large bulk measurements of brain activity.

This study takes the novel step to employ *in vivo* fluorescent neuronal imaging to measure the effect of isoflurane on neuronal systems with single neuron resolution, enabling a level of analysis not previously possible. As such, it opens a new window in anesthetic research to bridge the gap between bulk measurement of large brain regions and molecular studies of anesthetic action. By focusing on the well-defined command interneuron circuitry in *C. elegans,* the effects of anesthesia on a distinctly simple well-defined neuronal system are measured directly. Exposure to isoflurane induces randomized, uncoordinated neuronal activity within an inherently a well-organized circuit. In support of the original hypothesis, the quantification of correlations between neurons (Figure 4), spectral analysis of neuronal dynamics (Figure 5), as well as the entropy and multi-information of the neuronal signals (Table 1A) demonstrate that randomized dyssynchrony in neuronal signaling corresponds with the anesthetic state. Further expansion of these imaging techniques to pan-neuronal imaging, now possible in *C. elegans*, as well as application in other model systems, will prove informative in determining to what degree the effects observed here are conserved throughout the entire nervous system and ultimately defining the anesthetic mechanism of action on neuronal systems.

Acknowledgments

Financial Support:

NIH R01 GM121457

NIH R01 GM084491

NIH UL1 TR001430

Departmental support

C. elegans strains were obtained from Caenorhabditis Genetics Center (CGC, University of Minnesota). Fluorescence imaging was performed within the BUSM Confocal Microscope Facility, directed by Professor Vickery Trinkaus-Randall.

References

1. Hudson AE, Pryor KO. Integration and Information: Anesthetic Unconsciousness Finds a New Bandwidth. Anesthesiology. 2016; 125:832–834. [PubMed: 27617691]

2. White JG, Southgate E, Thomson JN, Brenner S. The structure of the nervous system of the nematode Caenorhabditis elegans. Philos Trans R Soc Lond B Biol Sci. 1986; 314:1–340. [PubMed: 22462104]

3. Chalfie M, Sulston JE, White JG, Southgate E, Thomson JN, Brenner S. The neural circuit for touch sensitivity in Caenorhabditis elegans. J Neurosci. 1985; 5:956–64. [PubMed: 3981252]

4. Shtonda BB, Avery L. Dietary choice behavior in Caenorhabditis elegans. J Exp Biol. 2006; 209:89–102. [PubMed: 16354781]

5. Ardiel EL, Rankin CH. An elegant mind: learning and memory in Caenorhabditis elegans. Learn Mem. 2010; 17:191–201. [PubMed: 20335372]

6. Morgan PGKEB, Sedensky MM. C. elegans and volatile anesthetics. In: Maricq AVMS, editorWormbook. 2007.

7. Morgan PG, Cascorbi HF. Effect of anesthetics and a convulsant on normal and mutant Caenorhabditis elegans. Anesthesiology. 1985; 62:738–44. [PubMed: 4003794]

8. Kato S, Kaplan HS, Schrodel T, Skora S, Lindsay TH, Yemini E, Lockery S, Zimmer M. Global Brain Dynamics Embed the Motor Command Sequence of Caenorhabditis elegans. Cell. 2015; 163:656–69. [PubMed: 26478179]

9. Schrodel T, Prevedel R, Aumayr K, Zimmer M, Vaziri A. Brain-wide 3D imaging of neuronal activity in Caenorhabditis elegans with sculpted light. Nat Methods. 2013; 10:1013–20. [PubMed: 24013820]

10. Venkatachalam V, Ji N, Wang X, Clark C, Mitchell JK, Klein M, Tabone CJ, Florman J, Ji H, Greenwood J, Chisholm AD, Srinivasan J, Alkema M, Zhen M, Samuel AD. Pan-neuronal imaging in roaming Caenorhabditis elegans. Proc Natl Acad Sci U S A. 2015

11. Nguyen JP, Shipley FB, Linder AN, Plummer GS, Liu M, Setru SU, Shaevitz JW, Leifer AM. Whole-brain calcium imaging with cellular resolution in freely behaving Caenorhabditis elegans. Proc Natl Acad Sci U S A. 2015

12. Roberts WM, Augustine SB, Lawton KJ, Lindsay TH, Thiele TR, Izquierdo EJ, Faumont S, Lindsay RA, Britton MC, Pokala N, Bargmann CI, Lockery SR. A stochastic neuronal model predicts random search behaviors at multiple spatial scales in C. elegans. Elife. 2016:5.

13. Chen TW, Wardill TJ, Sun Y, Pulver SR, Renninger SL, Baohan A, Schreiter ER, Kerr RA, Orger MB, Jayaraman V, Looger LL, Svoboda K, Kim DS. Ultrasensitive fluorescent proteins for imaging neuronal activity. Nature. 2013; 499:295–300. [PubMed: 23868258]

14. Mellem JE, Brockie PJ, Madsen DM, Maricq AV. Action potentials contribute to neuronal signaling in C. elegans. Nat Neurosci. 2008; 11:865–7. [PubMed: 18587393]

15. Lockery SR, Goodman MB. The quest for action potentials in C. elegans neurons hits a plateau. Nat Neurosci. 2009; 12:377–8. [PubMed: 19322241]

16. Chartrand R. ISRN Applied Mathematics 2011. 2011. Numerical differentiation of noisy, nonsmooth data.

17. Bedard C, Kroger H, Destexhe A. Modeling extracellular field potentials and the frequency-filtering properties of extracellular space. Biophys J. 2004; 86:1829–42. [PubMed: 14990509]

18. Tononi G. Consciousness as integrated information: a provisional manifesto. Biol Bull. 2008; 215:216–42. [PubMed: 19098144]

19. Lee U, Ku S, Noh G, Baek S, Choi B, Mashour GA. Disruption of frontal-parietal communication by ketamine, propofol, and sevoflurane. Anesthesiology. 2013; 118:1264–75. [PubMed: 23695090]

20. Studený M, Vejnarová J. Learning in graphical models. Springer; 1998. The multiinformation function as a tool for measuring stochastic dependence; 261–297.

21. Gray JM, Hill JJ, Bargmann CI. A circuit for navigation in Caenorhabditis elegans. Proc Natl Acad Sci U S A. 2005; 102:3184–91. [PubMed: 15689400]

22. Schwender D, Daunderer M, Mulzer S, Klasing S, Finsterer U, Peter K. Spectral edge frequency of the electroencephalogram to monitor “depth” of anaesthesia with isoflurane or propofol. Br J Anaesth. 1996; 77:179–84. [PubMed: 8881621]

23. Quintana A, Morgan PG, Kruse SE, Palmiter RD, Sedensky MM. Altered anesthetic sensitivity of mice lacking Ndufs4, a subunit of mitochondrial complex I. PLoS One. 2012; 7:e42904. [PubMed: 22912761]

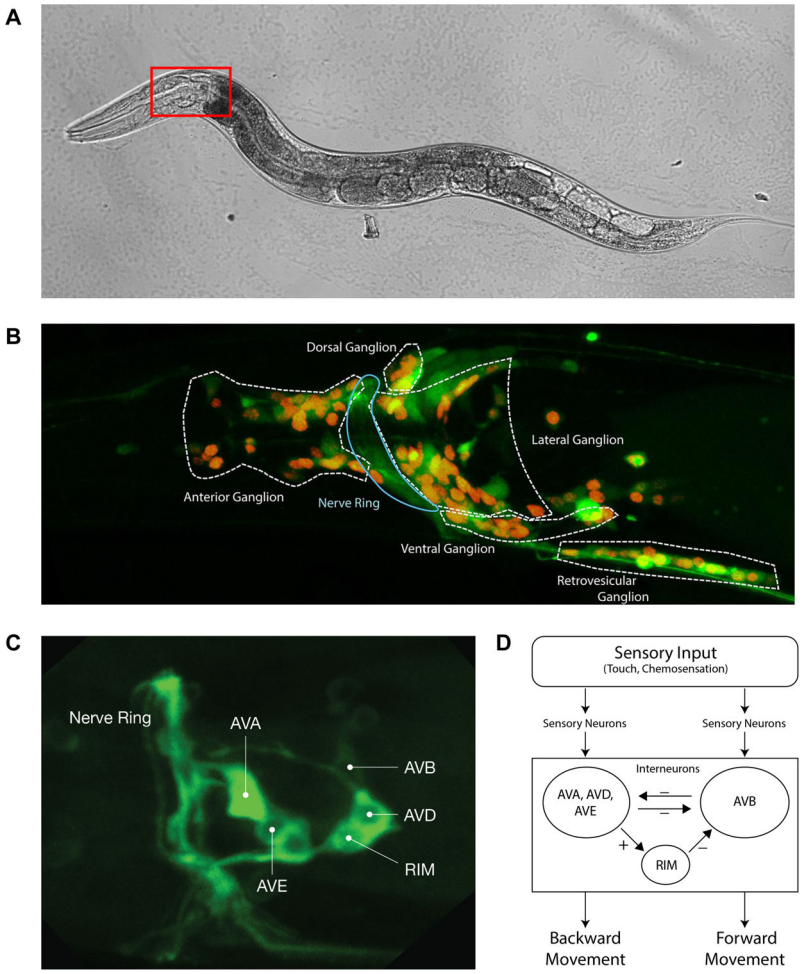

Figure 1. Gross and functional neuroanatomy of the *C. elegans* model

A. *C. elegans*, standard bright field microscopy.

B. Confocal fluorescent image of the *C. elegans* head, demonstrating the expression of a pan-neuronal calcium-sensitive green marker (GCaMP) and a red nuclear marker (RFP). Representative of the region of interest marked in Figure 1A.

C. Neurons AVA, AVB, AVD, AVE and RIM identified under selective expression of GCaMP in the QW1574 worm.

D. Schematic diagram of the *C. elegans* neuronal circuit controlling forward/backward crawling.

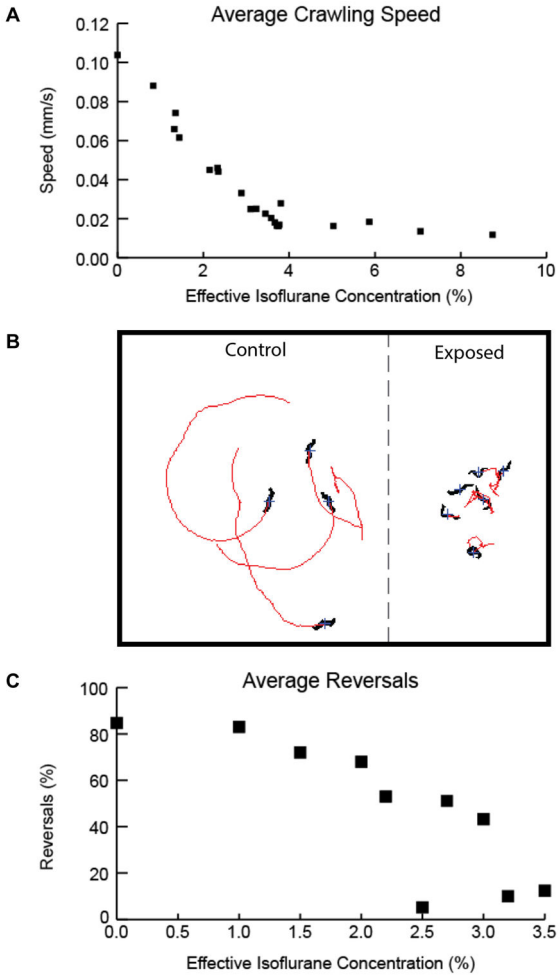

Figure 2. Disruption of *C. elegans* behavior under isoflurane anesthesia

A. Average crawling speed at indicated levels of isoflurane.

B. Examples of crawling tracks with and without exposure to isoflurane.

C. Touch avoidance response measured as % of animals responding (crawling reversal) to a mechanical buzz at indicated levels of isoflurane.

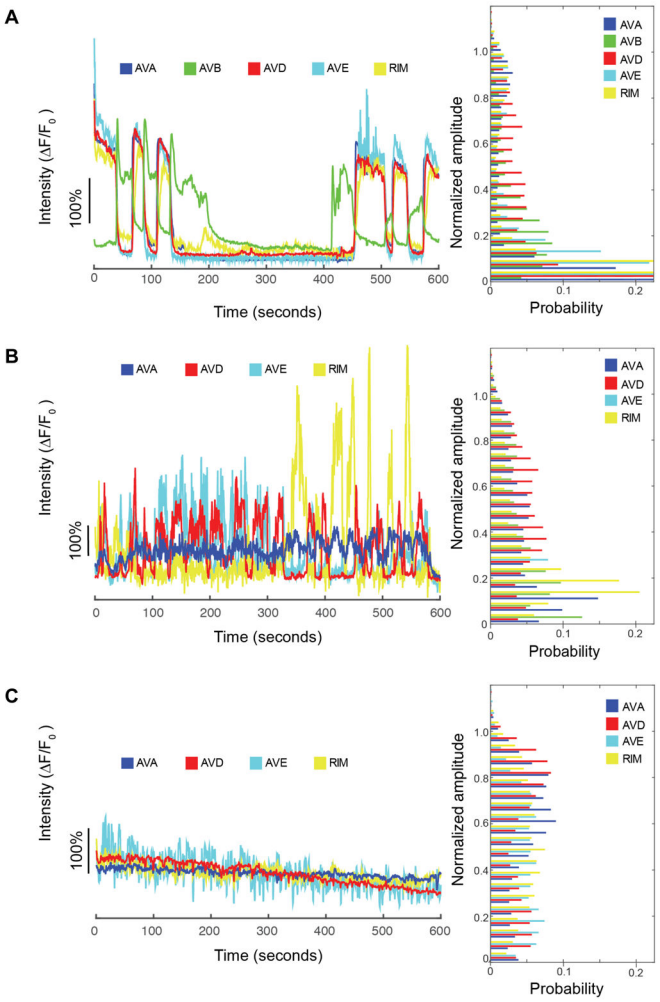

Figure 3. Functional imaging of the command interneurons AVA, AVD, AVE and RIM, showing spontaneous activity at varying levels of anesthesia. Example traces of individual animals are displayed (left), along with a histogram (right) of the normalized neuronal signals across all animals measured under that condition. The oppositional activity of AVB is shown in the unanesthetized state

A. Control, unanesthetized (0%vol isoflurane)

B. At moderate levels of anesthesia (4%vol isoflurane)

C. At deep levels of anesthesia (8%vol isoflurane)

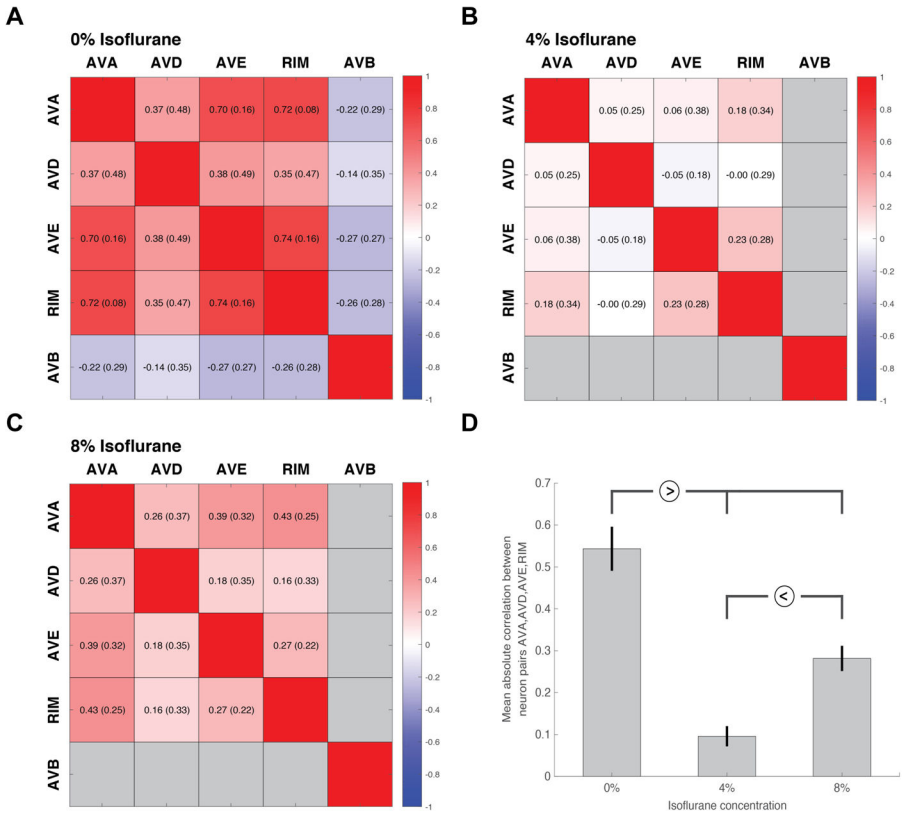

Figure 4. Correlation heatmaps displaying the correlation coefficient (SD) between neurons AVA, AVD, AVE and RIM at varying levels of anesthesia. AVB is shown only in the unanesthetized state

A. Control, unanesthetized (0%vol isoflurane)

B. At moderate levels of anesthesia (4%vol isoflurane)

C. At deep levels of anesthesia (8%vol isoflurane)

D. The averaged absolute correlation value between neuron pairs AVA, AVD, AVE and RIM across all worms measured at each condition. (Separable with statistical significance as shown.)

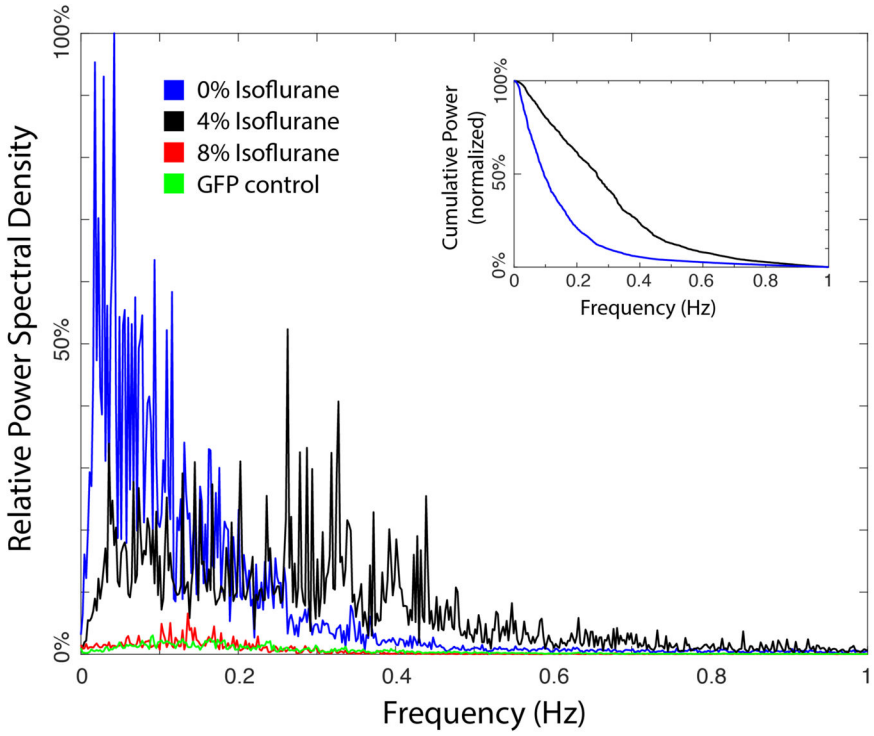

Figure 5. Mean power spectra of neuronal dynamics at varying levels of anesthesia

Mean power spectra were measured across all neurons imaged at 0%vol, 4%vol, 8%vol isoflurane. In addition, measurements from animals expressing GFP in the imaged neurons are displayed as controls. Insert: The cumulative normalized power spectra measured at 0%vol and 4%vol isoflurane.

Table 1A

Information content of the neuronal traces under varying depths of isoflurane anesthesia (Figure 3) as expressed in terms of the Shannon entropy (*H*, bits) after discretization into quartiles. *H*(Joint) is the joint entropy *H*(AVA, AVD, AVE, RIM). The maximum possible value of H for individual neurons is 2, and for the joint entropy is 8. The *multi-information*, *M*, is a representation of the degree of mutual information contained within the neuronal network and will fall towards zero as the activity of the involved neurons becomes random and independent.

Isoflurane	*n* worms	*H*(AVA)	*H*(AVD)	*H*(AVE)	*H*(RIM)	*H*(Joint)	*M*	M_{max}	*M* as % of M_{max}
0%	10	1.16	1.60	1.20	1.12	3.52	1.56	3.49	44.7%
4%	12	1.70	1.78	1.59	1.15	5.83	0.41	4.45	9.1%
8%	9	1.83	1.95	1.70	1.79	6.45	0.83	5.33	15.6%

Table 1B

The multi-information M, when calculated on a per-worm basis, can be expressed as an average and standard deviation at each of the levels of isoflurane anesthesia. Note that calculating entropy on a per-worm basis tends to underestimate the joint entropy due to undersampling and hence artifactually increase the multi-information M compared to Table 1A. Nevertheless, application of a two-sample t-test shows that both isoflurane 4% and isoflurane 8% have a lower multi-information than isoflurane 0% with statistical significance (**). The difference between isoflurane 4% and 8% is not significant.

Isoflurane	*n* worms	Average M/M_{max} as %	Standard Deviation
0%	10	61.7 %	16.8
4%	12	29.0 % **	16.1
8%	9	39.6 % **	9.2